Demystifying compressed top squark region with kinematic variables

Partha Konar,[1,*] Tanmoy Mondal,[1,2,†] and Abhaya Kumar Swain[1,‡]

[1] *Physical Research Laboratory (PRL), Ahmedabad - 380009, Gujarat, India*
[2] *Regional Centre for Accelerator-based Particle Physics, Harish-Chandra Research Institute, HBNI, Chhatnag Road, Jhusi, Allahabad - 211019, India*

(Dated: December 13, 2016)

We investigate the usefulness of different kinematic variables sensitive to the compressed mass region, and propose a search strategy considering phenomenological supersymmetric scenario where the top squark undergoes a four-body decay due to it's extremely narrow mass difference with the lightest supersymmetric particle. While Large Hadron Collider has already excluded large parameter space in supersymmetry, nearly degenerate mass spectrum has significantly hindered the search with a weaker bound. Considering a challenging but relatively clean decay channel, we demonstrate that one can effectively restrain the significant background from top and substantially improve the present limit with 13 TeV data.

PACS numbers: 14.80.Ly,12.60.Jv,13.85.-t

arXiv:1612.03269v1 [hep-ph] 10 Dec 2016

Introduction:- The Large Hadron Collider (LHC) with its enhanced center of mass energy and the luminosity, holds phenomenal potential to search for physics beyond the Standard Model (BSM). Among possible extensions, the supersymmetry (SUSY) is undoubtedly the most appealing theory waiting to be discovered at the LHC. It not only unifies the gauge couplings exactly, it also stabilizes the Higgs boson mass against large quantum correction. Lightest supersymmetric particle (LSP) in a R-parity conserved SUSY often considered as a possible dark matter candidate. The natural SUSY with light top squark mass (≤ 1 TeV) is favourable. Searching for R-parity conserving natural SUSY at the LHC is challenging bestowed upon the final states involving at least two invisible massive LSPs which escape the detection. There are many dedicated prescriptions discussed in the literature using which the LHC severely constrained the light top squark mass. Direct searches exclude top squark mass ($m_{\tilde{t}}$) below 800-900 GeV when the top squark decays to a top quark and a neutralino [1, 2].

Since we are lacking any hints yet of the grand design towards the expected pattern of SUSY masses, our blind phenomenological searches bring us certain interesting parameter space where LHC exclusion bound is significantly poor. This region of SUSY mass spectrum is known as compressed region, where the mass difference between top squark ($\tilde{t}$) and the LSP, commonly taken as neutralino (χ) is small. Depending upon the degree of smallness in this gap, different decay channels and thus scope for various search schemes arise. By itself, this small mass gap leads to the production of soft particles making it very difficult to identify them in the detector. Moreover, the massive neutralinos carry the highest fraction of the top squark momentum and each of them flies in the opposite direction leading to cancellation of the transverse momentum between them. So, the characteristic SUSY signature of large missing transverse momentum ($\not{E}_T$) is no more potent enough to control dominant backgrounds from the SM. Hence, new and better suited kinematic variables need to be studied keeping these challenges in mind.

In order to detect soft particles from the signal region and also to produce a sizable amount of missing transverse momenta, one requires to have reasonably high P_T initial state radiation (ISR) jet(s) accompanying the top squark pair production. This essentially boost this pair system at a price of reduced cross section. Now since the decay products from top squark includes both visible and invisible particles, any constructed observable, lacking the full phase space information, exhibits kinematic singularities in the observable phase space [3]. Once constructed, these observables can exhibit strikingly different behavior which one can rely upon to build efficient handle over extremely large backgrounds. The purpose of this study is two fold: first to demonstrate the capability of such array of variables in the context of compressed top squark scenario and secondly to substantiate that one can effectively restrain the significant background from top and substantially improve/complement the present limit with 13 TeV data.

We choose the rather challenging signal region where the mass difference between the top squark and LSP neutralino is smaller than the mass of $W-$boson and a $b-$quark combined. Consequently, the top squark can decay via the flavor changing neutral current through loop-induced two-body decay mode $\tilde{t} \to c\,\chi$ or the four-body mode $\tilde{t} \to b\,f\,f'\,\chi$ [4–6]. Recently the ATLAS and CMS collaborations also analyzed these channels with a soft lepton detection capability. Although the bounds on top squark mass in low mass gap is getting better, there are large parameter space remain unconstrained when the top squark and neutralino mass gap is closer to the $W-$boson mass. In this letter we focus mainly on this region and exploit the suitable kinematic variables to constrain the parameter space still untouched by the ATLAS and the CMS collaborations.

Existing top squark four-body searches:- Searches carried out by the LHC collaborations are of two kind. Monojet+$\not{E}_T$ search strategy rely on hard ISR jet(s) together with large $\not{E}_T$ which helps to tag the events. Since none of the decay products of the top squark are reconstructed at the detector, this channel is sensitive when the mass gap is small around 20 GeV. The four-body decay mode was searched by ATLAS [7] with 8 TeV LHC data, whereas CMS has searched in full hadronic decay mode including a b-tagged jet along with multiple jets associated with large $\not{E}_T$ using 13 TeV data. Top squark masses up to 450 GeV was probed for neutralino mass of 430 GeV [8]. Importance of b-tagging was demonstrated in [9].

In the second strategy with lepton(s)+jets+$\not{E}_T$, at least one lepton is reconstructed and consequently larger mass gap was probed. With 8 TeV data both CMS [10] and ATLAS [11] has searched compressed region with only one lepton in the final state. With the new 13 TeV data CMS moved one step further and explored the region with both one-lepton [12] and two-leptons [13] in the final state. The leptons with $p_T > 5$ GeV were reconstructed with particle-flow algorithm which helps to search for the low mass gap region with leptonic channel which we also used to project our results. Assuming a 100% branching ratio of the four-body decay,and prompt decay top squark masses below 330 GeV are excluded at 95% confidence level for a mass difference to the LSP of about 25 GeV in one-lepton search [12], whereas the limit from two-lepton search is 360 GeV with $m_{\tilde{t}} - m_{\chi} = 30$ GeV [13]. For the two-lepton channel the ratio $\not{E}_T/H_T$ was used to minimize the QCD background. H_T is the scalar sum of all the jet transverse momenta. ATLAS has not yet studied the region with new 13 TeV data.

Apart from the four-body decay mode, the two-body decay $\tilde{t} \rightarrow c\,\chi$ was also searched by the experimental collaborations. Since the charm quark can not be tagged efficiently inside a jet, both the CMS [14] and ATLAS [7, 15] rely on the monojet+$\not{E}_T$ signal with 8 TeV energy. With new 13 TeV data CMS used the α_T variable and the limit on top squark mass goes up to 400 GeV with neutralino mass of 310 GeV. Conventional monojet+$\not{E}_T$ search with 13 TeV data provide limit on top squark mass of 323 GeV as reported by the ATLAS collaboration [16].

Note that all the analysis were done assuming 100% branching ratio to either four-body or two-body decay mode. In the CMS analysis [17] it was assumed that top squark branching ratio is 50% to both two-body and four-body channel and in that case the limit on top squark mass is 360 GeV [17] with the α_T analysis.

Apart from the experimental searches, several novel methods were proposed to search for the compressed region at the collider [9, 18–42]. Recently, an interesting but simple kinematic variable R_M [43] was proposed which suited with the compressed region of SUSY. It needs a hard ISR jet to be produced with top squark pair

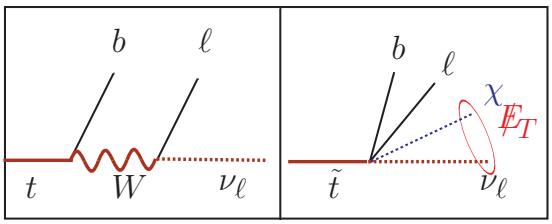

FIG. 1: The right panel shows the top squark four-body decay producing top and $W-$boson off-shell. The left panel shows the top decay via leptonic channel.

and is defined as the ratio between missing transverse momenta and the ISR jet transverse momenta. This variable peaks at neutralino and top squark mass ratio $(m_{\chi}/m_{\tilde{t}})$ while the background falls exponentially. Subsequently, it is noticed [44] that the presence other sources of missing energy which may come from the neutrino(s) of leptonic decay modes, this variable spreads around the peak leading to the reduction of the signal and background discriminating power. While for semi-leptonic decay, the neutrino contribution can be subtracted and the R_M variable behavior restored but for dileptonic decay channel separation of neutrino contribution is not possible.

Kinematic and invariant mass variables:- In order to demonstrate the efficacy of kinematic features, we consider a challenging but relatively clean decay channel of the top squark, the dileptonic channel,

$$PP \rightarrow \tilde{t} + \tilde{t}^* \rightarrow \chi_1^0\, b\, \ell^+\, \bar{\nu_\ell} + \chi_1^0\, \bar{b}\, \ell^-\, \nu_\ell, \qquad (1)$$

along with ISR jet(s). Evidently, the signal we consider for our analysis contains two lepton, at least one b-tagged jet, one or more high P_T ISR jet(s) and large missing transverse momenta. Since all the leptons and $b-$quarks are mostly soft, it is not much economical to tag both the $b-$jets due to low b-tagging efficiency $(40-50\%)$, which peaks around $70-80\%$ when p_T is 70-100 GeV. As stated earlier, the main background for this signal region is the top pair production in the dileptonic channel.

The cascade decay topology for both the signal and background is shown in the Fig. 1 where the left panel is for top decay while right panel is for top squark decay. Although we take pair production for both the signal and the background, we only display one side of the decay topology since it is symmetric. We also consider the mass difference between the top squark and neutralino to be smaller than the $W-$boson mass, $\Delta M = m_{\tilde{t}} - m_{\chi} \leq m_W$. In this scenario both the top and subsequently the $W-$boson will be produced off-shell for the signal resulting the four-body decay, unlike the background top pair case which is sequential two-body decay. In the signal region, the two invisible particles, from each top squark decay, are combined to form an effective invisible particle as represented by the oval in Fig. 1 with invariant mass m_I.

These distinct kinematic topologies between the signal and the background empower one to look for different kinematic variables possessing characteristic observable singularities in phase space to discover or exclude the light top squark in the compressed region at the LHC. The kinematic variables which best incorporate the topology information are the ones having best discriminating power. For example, the invariant mass of the visible particles can be a good discriminator of the kinematic topology [45]. In our present example invariant mass of the b-tagged jet and the lepton, $M_{b\ell}$ can be utilized for maximizing the signal to background ratio. The distribution of the variable $M_{b\ell}$ has an endpoint which arises, as mentioned earlier, because of the singularity in the observable phase space. The full phase space does not include a singularity but observable phase space does as we measure a subset of event momenta [3]. The invariant mass $M_{b\ell}$ is a projection of full phase space on to the observable phase space and any folding in the full phase space resulted as a singularity (endpoint). Position of the edge of $M_{b\ell}$ distribution depends on the decay topology as,

$$M_{b\ell}^{max} = \begin{cases} \sqrt{m_{\tilde{t}}^2 - m_W^2}, & \text{for top background} \\ (m_{\tilde{t}} - m_I^{min}) = (m_{\tilde{t}} - m_\chi), & \text{for signal,} \end{cases} \quad (2)$$

after neglecting the neutrino mass. Therefore, for the background events, the position of endpoint of $M_{b\ell}$ distribution will be larger compared to the signal events which is confined within ΔM.

At this point, we also propose two new ratios possessing distinct facet specifically for the four-body decay of compressed region of SUSY. To motivate with concrete examples, one starts with a scenario with mass difference between top squark and neutralino being tiny, such as, $\Delta M = 5$ GeV. The transverse momenta of top squark and $b-$jet are related as $P_T^{\tilde{t}} = (m_{\tilde{t}}/m_b)P_T^b$. One can also write similar equation for the corresponding lepton from the decay and finally, using both these relations we construct two new ratios,

$$R_{bE} = \frac{\sum P_T^{b_i}}{\not{E}_T}, \qquad R_{\ell E} = \frac{\sum P_T^{\ell_i}}{\not{E}_T}. \quad (3)$$

It is easy to follow that for the signal region R_{bE} peaks at the mass ratio (m_b/m_χ), whereas $R_{\ell E}$ peaks at $(m_\ell/m_\chi) \approx 0$. These two interesting ratios serve much better in comparison to R_M in the dileptonic decay channel exploring the top squark four-body decay scenario. While R_{bE} performance in the four-body decay region remains robust, the $R_{\ell E}$ distribution starts spreading for larger ΔM, *e.g.*, typically for 50 GeV or more. Although we have only one b-tagged jet in the signal region, we propose to use the ratio of one $b-$jet and missing transverse momentum and still having a good discriminating capability.

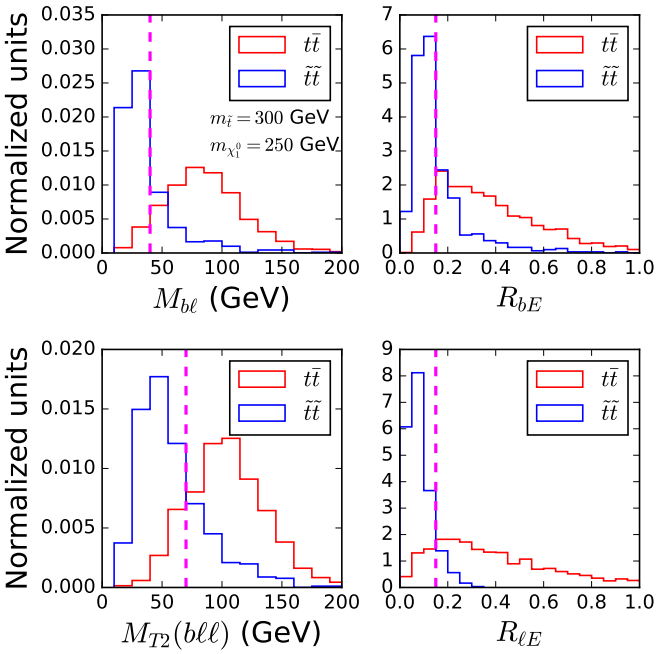

FIG. 2: The distribution of four variables $M_{b\ell}$, R_{bE}, $R_{\ell E}$ and $M_{T2}(b\ell\ell)$ are shown here (clockwise). The Red and blue distributions are for the signal and background events, respectively. The distribution was simulated for $\Delta M = 50$ GeV with top squark mass, $m_{\tilde{t}} = 300$ GeV.

Our final observable is the stransverse mass $M_{T2}(b\ell\ell)$ of the $b-$jet and two leptons which also favored with good discriminating power. Although the symmetric M_{T2} constructed from two $b-$jets and two-lepton subsystem would have been very useful, here we advocate to use the asymmetric $M_{T2}(b\ell\ell)$ which inherits nearly all the properties that of symmetric one, with an added benefit of larger statistics from tagging just one $b-$jet. By definition, M_{T2} distribution have a kinematic endpoint which depends on the decay topology. It is observed to have comparable efficiency with that of $M_{b\ell}$.

Event simulation and basic cuts:- We simulate the signal events using `MadGraph5` [46] for parton level event generation and those events were passed to `Pythia8` [47, 48] for hadronization and parton showering and finally detector level simulation is done in `Delphes3` [49] using the available ATLAS card. All the jets are reconstructed using anti-kT algorithm with $R = 0.4$ having $p_T > 20$ GeV. The highest p_T jet was tagged as the ISR jet and we have vetoed all the events where the ISR tagged jet was also b-tagged or $p_T(j_{ISR}) < 100$ GeV. Very hard ISR jet is not considered, to begin with, in comparison to usual compressed searches, to increase the available number of signal events for investigating our variables further. For all our analysis we have used the next-to-leading-order (NLO) plus next-to-leading-logarithm (NLL) top squark cross sections given by the LHC SUSY Cross Section Working Group [50, 51].

The main background for this signal is the $t\,\bar{t}$ events for which process generation and hadronization was done in `Pythia8` [47, 48] and `Delphes3` [49] was used for detector simulation. The predicted $t\bar{t}$ production cross section is $\sigma_{t\bar{t}} = 815.96$ pb as calculated with the Top++2.0 program to next-to-next-to-leading order in perturbative QCD, including soft-gluon resummation to next-to-next-to-leading-log order (see [52] and references therein), and assuming a top quark mass $m_t = 173.2$ GeV.

Since we are always very close to threshold production, the momentum carried away by the decay products of the top squark are proportional to the masses of the particles. Consequently, neutralino carries away most of the $p_T(\tilde{t})$ now giving rise to large missing momentum for top squark decay, whereas for top quark the momentum is shared more evenly and $\not{E}_T$ is comparably small. Hence, we choose a $\not{E}_T$ cut of 200 GeV to reduce significant amount of background events including the QCD multi-jet backgrounds. In the same spirit we have included another variable $\not{E}_T/M_{eff} > 0.3$ where M_{eff} is the scalar sum of all momentum including ISR. Large ratio ensures the fact that the missing energy is the principal component of the total transverse momentum.

Exploiting the fact that the ISR will be approximately in the opposite direction to the $\not{E}_T$, we introduce additional cut that $|\phi(ISR) - \phi(\not{E}_T) - \pi| < 0.4$. This will also significantly diminish the enormous QCD background. To minimize the effect of jet mis-measurement contributing into $\not{E}_T$ we also demand that $|\phi(j) - \phi(\not{E}_T)| > 0.2$ for all jets other than the ISR.

Results:- Using the simulated events which passed all the basic selection cuts described above we have plotted all four pivotal variables for both signal and background $t\bar{t}$ events in Fig. 2. The signal events for this demonstration are generated with top squark mass 300 GeV and neutralino mass 250 GeV. In all the panels red distribution is for the background $t\bar{t}$ process and blue histograms are for the signal events. Also, with a vertical magenta line we have shown the upper limit we took for these variables to maximize signal over the background. As we can see both the kinematic variables R_{bE} and $R_{\ell E}$ falls sharply for the signal events whereas the background $t\bar{t}$ distribution is rather flat. As described before this is due to large $\not{E}_T$ and very soft leptons/$b-$jets originating from the decay of the top squark. Here these two plots are for $\Delta M = 50$ GeV and with decreasing ΔM, the variable $R_{\ell E}$ shifts towards left which is expected by construction. The ratio R_{bE} shows a little higher value because of two reasons; we are taking just one $b-$jet contribution and also due to the fact that there are chances that the origin of $b-$jet is not from the top squark decay.

In Fig. 2 we also plotted two mass variables namely the invariant mass of $b\ell$ system $M_{b\,\ell}$ and the stransverse mass distribution M_{T2} of the $b\ell\ell$ asymmetric subsystem setting the input trial invisible mass as our trivial choice, zero. Although we have not used the $M_{T2}(b\ell\ell)$ variable

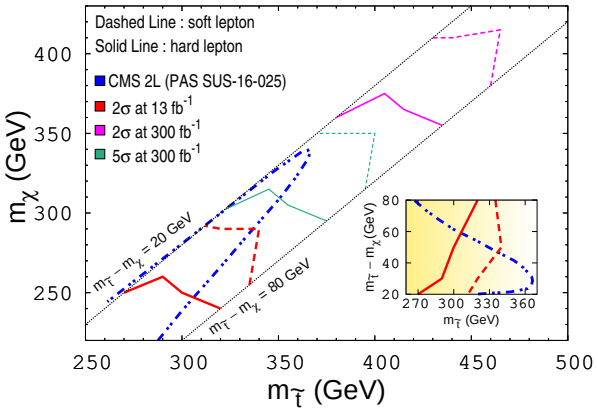
Dashed Line : soft lepton
Solid Line : hard lepton
CMS 2L (PAS SUS-16-025)
2σ at 13 fb-1
2σ at 300 fb-1
5σ at 300 fb-1
mχ (GeV)
mt̃ (GeV)
mt̃ − mχ = 20 GeV
mt̃ − mχ = 80 GeV
mt̃ − mχ (GeV)

FIG. 3: Exclusion limit with 13 fb^{-1} and 300 fb^{-1} data as well as discovery plot for 300 fb^{-1} data are shown with two different lepton $p_T(\ell)$ criteria. Inset shows exclusion limit in $m_{\tilde{t}} - \Delta M$ plane with 13.3 fb^{-1} luminosity using same legends.

for present analysis, it was also tested to a good discriminator with $M_{T2}(b\ell\ell) < 70$ GeV is signal rich region. One can notice that for signals most of the events are having smaller invariant mass $M_{b\ell}$ compared to the background making this a good discriminator. The $M_{b\ell}$ distribution for signal has a tail instead of endpoint at ΔM, this is because of the detector resolution and other realistic effects. There are two invariant masses possible using two leptons and one $b-$quark and we take the smaller one among them.

In order to maximize signal to background ratio we optimized the event selection cuts as: (i) $M_{b\ell} < 40$ (60) GeV, (ii) $R_{bE} < 0.15$ (0.1), and (iii) $R_{\ell E} < 0.15$ (0.3). The numbers in the parentheses are the cut used for $\Delta M = 80$ GeV which is different from the cuts used for other smaller ΔM values below 50 GeV. This is due to the fact that at this mass difference the $W-$boson is on-shell and effectively the lepton coming from $W-$boson becomes more energetic whereas the $b-$quark becomes softer. This effectively decreases the cut for R_{bE} and increases the cut value on $R_{\ell E}$ for 80 GeV mass difference.

Equipped with the optimized variables and event selection criteria we analyze the signal as well as background events, and plotted the significance plot for 13 TeV LHC with 13 and 300 fb^{-1} data in Fig. 3. For 2σ significance we use the formula $\mathcal{S} = S/\sqrt{S+B}$ and for 5σ the corresponding formula is $S/\sqrt{B}$ where $S(B)$ stands for number of signal(background) events at a particular integrated luminosity. The blue (dash-dot) curve shows the state-of-the-art limit on $\tilde{t}$ mass coming from dilepton search as presented by the CMS collaboration [13]. As we can see the limit is poor for larger mass difference and drops down pretty fast as we move towards the $m_{\tilde{t}} - m_\chi = m_W$ boundary. The red solid and red dashed curve show our exclusion limit at 13 TeV LHC with $13 fb^{-1}$ data. The two curves are for two different

lepton p_T criteria. In one case we have considered leptons with moderately high p_T (> 10 GeV) and the corresponding limit is represented by the solid curves. For an optimistic scenario, inspired by the CMS study [12, 13], we also provide projected plot with soft lepton criteria considering p_T threshold at 5 GeV and the corresponding limit is shown in dashed curves. Evidently new kinematic and mass variables works rather well for this region of parameter space, particularly in higher mass gap side our search channel provides a limit better than the existing CMS search. In the inset of Fig. 3 we have shown the results for luminosity of $13 fb^{-1}$ in $m_{\tilde{t}} - \Delta M$ plane. It is clear that the larger mass gap region can effectively be probed using the new variables proposed here.

We propose to use these variables for dileptonic channel at the LHC which will boost the experimental limit. Also, we exhibit the limits for 13 TeV LHC with an integrated luminosity of 300 fb^{-1}. The magenta curve shows 2σ exclusion limits whereas the green curve shows 5σ discovery potential. With our proposed variables at 13 TeV with 13 fb^{-1} data we can exclude top squark up to 320 GeV with neutralino mass 240 GeV and with interesting luminosity of 300 fb^{-1} data the limit on top squark can go up to 435 GeV with $m_\chi = 355$ GeV. Also, it is possible to discover the much sought top squark with 300 fb^{-1} data if the top squark lies below 375 GeV with a mass gap of 80 GeV.

Conclusion and discussion:- In this letter, we consider the degenerate top squark with the lightest neutralino whose production leads to the four-body decay of the top squark. Among decay channels the di-leptonic mode, despite being experimentally cleaner and more reliable search channel, is also challenging because of two additional neutrinos present in the final state. We proposed suitable kinematic variables which best exploit the decay topology information producing the kinematic end points. Our observables include invariant mass, stransverse mass, and two new ratios, to discriminate the signal four-body decay channel with sequential two-body decay expected from the background. With these variables the existing limit can be extended up to 335 GeV for mass gap of 80 GeV with current luminosity ($13 fb^{-1}$) of LHC at 95% confidence level in comparison to the recent CMS limit of 270 GeV. Hence, these interesting variables can be included to enhance the observables capability by LHC experimental collaborations. Also as a complementary channel along with the existing limits, prescribed search channel can provide the access of the parameter regions otherwise left out for the future compressed top squark search.

Acknowledgments.— This work was supported by the Physical Research Laboratory (PRL), Department of Space (DOS), India. T.M. acknowledge the funding available from the Department of Atomic Energy, Government of India, for the Regional Centre for Accelerator based Particle Physics (RECAPP), Harish-Chandra Research Institute.

* Electronic address: konar@prl.res.in
† Electronic address: tanmoym@prl.res.in
‡ Electronic address: abhaya@prl.res.in

[1] Tech. Rep. ATLAS-CONF-2016-050 (CERN, Geneva, 2016).
[2] Tech. Rep. CMS-PAS-SUS-16-028 (CERN, Geneva, 2016).
[3] I.-W. Kim, Phys. Rev. Lett. **104**, 081601 (2010), arXiv:0910.1149 [hep-ph] .
[4] K.-i. Hikasa and M. Kobayashi, Phys. Rev. **D36**, 724 (1987).
[5] C. Boehm, A. Djouadi, and Y. Mambrini, Phys. Rev. **D61**, 095006 (2000), arXiv:hep-ph/9907428 [hep-ph] .
[6] M. Muhlleitner and E. Popenda, JHEP **04**, 095 (2011), arXiv:1102.5712 [hep-ph] .
[7] G. Aad *et al.* (ATLAS), Phys. Rev. **D90**, 052008 (2014), arXiv:1407.0608 [hep-ex] .
[8] Tech. Rep. CMS-PAS-SUS-16-029 (CERN, Geneva, 2016).
[9] G. Ferretti, R. Franceschini, C. Petersson, and R. Torre, Phys. Rev. Lett. **114**, 201801 (2015), arXiv:1502.01721 [hep-ph] .
[10] V. Khachatryan *et al.* (CMS), Phys. Lett. **B759**, 9 (2016), arXiv:1512.08002 [hep-ex] .
[11] G. Aad *et al.* (ATLAS), JHEP **11**, 118 (2014), arXiv:1407.0583 [hep-ex] .
[12] Tech. Rep. CMS-PAS-SUS-16-031 (CERN, Geneva, 2016).
[13] Tech. Rep. CMS-PAS-SUS-16-025 (CERN, Geneva, 2016).
[14] V. Khachatryan *et al.* (CMS), JHEP **06**, 116 (2015), arXiv:1503.08037 [hep-ex] .
[15] G. Aad *et al.* (ATLAS), Eur. Phys. J. **C75**, 510 (2015), [Erratum: Eur. Phys. J.C76,no.3,153(2016)], arXiv:1506.08616 [hep-ex] .
[16] M. Aaboud *et al.* (ATLAS), Phys. Rev. **D94**, 032005 (2016), arXiv:1604.07773 [hep-ex] .
[17] V. Khachatryan *et al.* (CMS), (2016), arXiv:1611.00338 [hep-ex] .
[18] C.-L. Chou and M. E. Peskin, Phys. Rev. **D61**, 055004 (2000), arXiv:hep-ph/9909536 [hep-ph] .
[19] S. P. Das, A. Datta, and M. Guchait, Phys. Rev. **D65**, 095006 (2002), arXiv:hep-ph/0112182 [hep-ph] .
[20] M. Carena, A. Freitas, and C. E. M. Wagner, JHEP **10**, 109 (2008), arXiv:0808.2298 [hep-ph] .
[21] S. Bornhauser, M. Drees, S. Grab, and J. S. Kim, Phys. Rev. **D83**, 035008 (2011), arXiv:1011.5508 [hep-ph] .
[22] M. A. Ajaib, T. Li, and Q. Shafi, Phys. Rev. **D85**, 055021 (2012), arXiv:1111.4467 [hep-ph] .
[23] Y. Kats and D. Shih, JHEP **08**, 049 (2011), arXiv:1106.0030 [hep-ph] .
[24] B. He, T. Li, and Q. Shafi, JHEP **05**, 148 (2012), arXiv:1112.4461 [hep-ph] .
[25] M. Drees, M. Hanussek, and J. S. Kim, Phys. Rev. **D86**, 035024 (2012), arXiv:1201.5714 [hep-ph] .
[26] G. Belanger, M. Heikinheimo, and V. Sanz, JHEP **08**, 151 (2012), arXiv:1205.1463 [hep-ph] .
[27] D. S. M. Alves, M. R. Buckley, P. J. Fox, J. D.

Lykken, and C.-T. Yu, Phys. Rev. **D87**, 035016 (2013), arXiv:1205.5805 [hep-ph] .
[28] Z. Han, A. Katz, D. Krohn, and M. Reece, JHEP **08**, 083 (2012), arXiv:1205.5808 [hep-ph] .
[29] A. Choudhury and A. Datta, Mod. Phys. Lett. **A27**, 1250188 (2012), arXiv:1207.1846 [hep-ph] .
[30] H. Dreiner, M. Krämer, and J. Tattersall, Phys. Rev. **D87**, 035006 (2013), arXiv:1211.4981 [hep-ph] .
[31] K. Krizka, A. Kumar, and D. E. Morrissey, Phys. Rev. **D87**, 095016 (2013), arXiv:1212.4856 [hep-ph] .
[32] A. Delgado, G. F. Giudice, G. Isidori, M. Pierini, and A. Strumia, Eur. Phys. J. **C73**, 2370 (2013), arXiv:1212.6847 [hep-ph] .
[33] K. Hagiwara and T. Yamada, Phys. Rev. **D91**, 094007 (2015), arXiv:1307.1553 [hep-ph] .
[34] G. Belanger, D. Ghosh, R. Godbole, M. Guchait, and D. Sengupta, Phys. Rev. **D89**, 015003 (2014), arXiv:1308.6484 [hep-ph] .
[35] B. Dutta, W. Flanagan, A. Gurrola, W. Johns, T. Kamon, P. Sheldon, K. Sinha, K. Wang, and S. Wu, Phys. Rev. **D90**, 095022 (2014), arXiv:1312.1348 [hep-ph] .
[36] M. Czakon, A. Mitov, M. Papucci, J. T. Ruderman, and A. Weiler, Phys. Rev. Lett. **113**, 201803 (2014), arXiv:1407.1043 [hep-ph] .
[37] R. Gröber, M. M. Mühlleitner, E. Popenda, and A. Wlotzka, Eur. Phys. J. **C75**, 420 (2015), arXiv:1408.4662 [hep-ph] .
[38] K. Rolbiecki and J. Tattersall, Phys. Lett. **B750**, 247 (2015), arXiv:1505.05523 [hep-ph] .
[39] S. Macaluso, M. Park, D. Shih, and B. Tweedie, JHEP **03**, 151 (2016), arXiv:1506.07885 [hep-ph] .
[40] B. Kaufman, P. Nath, B. D. Nelson, and A. B. Spisak, Phys. Rev. **D92**, 095021 (2015), arXiv:1509.02530 [hep-ph] .
[41] A. Kobakhidze, N. Liu, L. Wu, J. M. Yang, and M. Zhang, Phys. Lett. **B755**, 76 (2016), arXiv:1511.02371 [hep-ph] .
[42] D. Goncalves, K. Sakurai, and M. Takeuchi, (2016), arXiv:1610.06179 [hep-ph] .
[43] H. An and L.-T. Wang, Phys. Rev. Lett. **115**, 181602 (2015), arXiv:1506.00653 [hep-ph] .
[44] H.-C. Cheng, C. Gao, L. Li, and N. A. Neill, JHEP **05**, 036 (2016), arXiv:1604.00007 [hep-ph] .
[45] W. S. Cho, D. Kim, K. T. Matchev, and M. Park, Phys. Rev. Lett. **112**, 211801 (2014), arXiv:1206.1546 [hep-ph] .
[46] J. Alwall, M. Herquet, F. Maltoni, O. Mattelaer, and T. Stelzer, JHEP **06**, 128 (2011), arXiv:1106.0522 [hep-ph] .
[47] T. Sjostrand, S. Mrenna, and P. Z. Skands, JHEP **05**, 026 (2006), arXiv:hep-ph/0603175 [hep-ph] .
[48] T. Sjostrand, S. Mrenna, and P. Z. Skands, Comput. Phys. Commun. **178**, 852 (2008), arXiv:0710.3820 [hep-ph] .
[49] J. de Favereau, C. Delaere, P. Demin, A. Giammanco, V. Lemaître, A. Mertens, and M. Selvaggi (DELPHES 3), JHEP **02**, 057 (2014), arXiv:1307.6346 [hep-ex] .
[50] "S. padhi (lhc susy cross section working group)," `https://twiki.cern.ch/twiki/bin/view/LHCPhysics/SUSYCrossSections`.
[51] C. Borschensky, M. Krämer, A. Kulesza, M. Mangano, S. Padhi, T. Plehn, and X. Portell, Eur. Phys. J. **C74**, 3174 (2014), arXiv:1407.5066 [hep-ph] .
[52] M. Czakon and A. Mitov, Comput. Phys. Commun. **185**, 2930 (2014), arXiv:1112.5675 [hep-ph] .